

## Research



**Cite this article:** Divi S, Ma X, Ilton M, St. Pierre R, Eslami B, Patek SN, Bergbreiter S. 2020 Latch-based control of energy output in spring actuated systems. *J. R. Soc. Interface* **17**: 20200070.  
<http://dx.doi.org/10.1098/rsif.2020.0070>

Received: 31 January 2020  
Accepted: 29 June 2020

**Subject Category:**  
Life Sciences—Engineering interface

**Subject Areas:**  
biomechanics, biomimetics

**Keywords:**  
spring-actuated systems, latching mechanisms, latch-mediated spring actuation, mechanical power amplification, latch

**Author for correspondence:**  
Sarah Bergbreiter  
e-mail: [sbergbre@andrew.cmu.edu](mailto:sbergbre@andrew.cmu.edu)

Electronic supplementary material is available online at <https://doi.org/10.6084/m9.figshare.c.5067107>.

# Latch-based control of energy output in spring actuated systems

Sathvik Divi<sup>1</sup>, Xiaotian Ma<sup>1</sup>, Mark Ilton<sup>2</sup>, Ryan St. Pierre<sup>1</sup>, Babak Eslami<sup>3</sup>, S. N. Patek<sup>4</sup> and Sarah Bergbreiter<sup>1</sup>

<sup>1</sup>Department of Mechanical Engineering, Carnegie Mellon University, Pittsburgh, PA 15213, USA

<sup>2</sup>Department of Physics, Harvey Mudd College, Claremont, CA 91711, USA

<sup>3</sup>Department of Mechanical Engineering, Widener University, Chester, PA 19013, USA

<sup>4</sup>Department of Biology, Duke University, Durham, NC 27708, USA

SD, 0000-0002-6028-3087; SB, 0000-0003-2735-0206

The inherent force–velocity trade-off of muscles and motors can be overcome by instead loading and releasing energy in springs to power extreme movements. A key component of this paradigm is the latch that mediates the release of spring energy to power the motion. Latches have traditionally been considered as switches; they maintain spring compression in one state and allow the spring to release energy without constraint in the other. Using a mathematical model of a simplified contact latch, we reproduce this instantaneous release behaviour and also demonstrate that changing latch parameters (latch release velocity and radius) can reduce and delay the energy released by the spring. We identify a critical threshold between instantaneous and delayed release that depends on the latch, spring, and mass of the system. Systems with stiff springs and small mass can attain a wide range of output performance, including instantaneous behaviour, by changing latch release velocity. We validate this model in both a physical experiment as well as with data from the Dracula ant, *Myrmica camillae*, and propose that latch release velocity can be used in both engineering and biological systems to control energy output.

## 1. Background

Latch-mediated spring actuation (LaMSA) mechanisms use latches to release energy stored in springs to generate motion [1]. Many small organisms employ these LaMSA mechanisms to circumvent the force–velocity trade-off in their muscles to achieve higher power output. Latches play a critical role in LaMSA systems by mediating the transition from stored spring potential energy to kinetic energy. A diversity of physical phenomena can act as a latch as outlined in [2], including contact (figure 1), fluids [3] and geometry [4–6]. Geometric latches encompass a variety of subcategories including over-centering latches [4] and agonist–antagonist muscle pairs [5]. In a simple model of these spring-actuated systems based on [2], motion is separated into distinct phases (figure 1). An actuator (e.g. motor, muscle) stores energy in a spring that is then held in place by a contact latch with a radius  $R$ . When the latch is removed (also by an actuator) with velocity  $v_L$ , this energy is quickly released.

By using LaMSA mechanisms, small and lightweight organisms achieve accelerations and velocities far beyond what their muscles and actuators can accomplish alone. Trap-jaw ants (mandible strike:  $64 \text{ m s}^{-1}$  at an average acceleration of the order of  $10^6 \text{ m s}^{-2}$ ) [7–13], mantis shrimp (predatory strike: up to  $31 \text{ m s}^{-1}$  at an average acceleration of the order of  $10^4 \text{ m s}^{-2}$ ) [14–18], froghoppers (jump:  $4.7 \text{ m s}^{-1}$  at an average acceleration of the order of  $10^3 \text{ m s}^{-2}$ ) [19,20], and even soft-bodied gall midges (jump:  $0.88 \text{ m s}^{-1}$  at an average acceleration on the order of  $880 \text{ m s}^{-2}$ ) [21] are just a few examples. Furthermore, LaMSA mechanisms are used in a variety of organisms for diverse applications ranging from prey capture and predator evasion, to jumping locomotion. Leaf closures of venus flytraps [22], nematocyst discharge by hydra [23], tongue

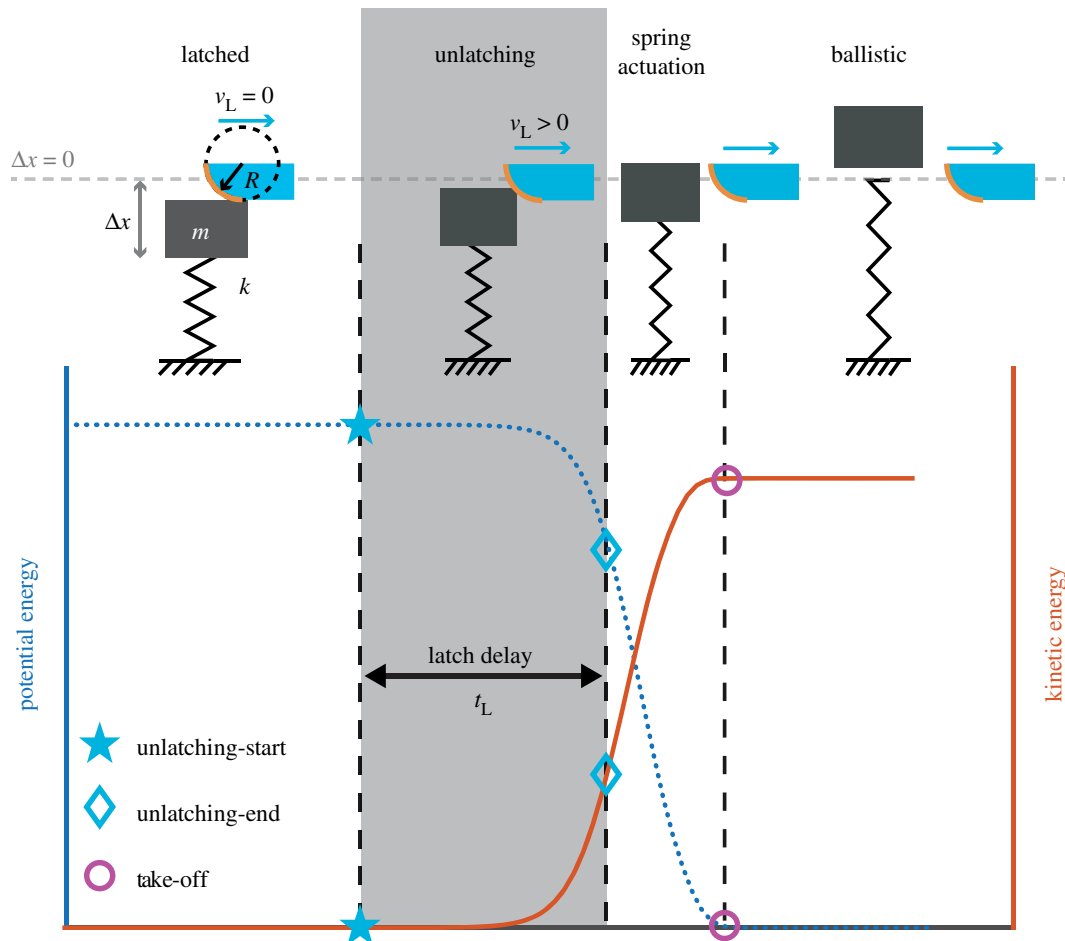


**Figure 1.** Model representation of a latch-mediated spring actuation (LaMSA) system incorporating a contact latch with a latch radius  $R$  (highlighted in orange) being pulled away at a velocity  $v_L$ . Phases involved in the transfer of energy in LaMSA systems are also shown. In the latched phase, the latch constrains a spring that has been previously compressed by distance  $\Delta x$  (by an actuator or external force not shown). The release of the latch with a velocity  $v_L > 0$  triggers the onset of spring expansion. In an instantaneous latch, there is no latch delay ( $t_L = 0$ ) and the system instantaneously moves to the spring actuation phase in which the spring expansion is unconstrained by the latch and depends solely on the mass–spring dynamics. In a delayed latch, an unlatching phase exists (grey region) in which the latch continues to constrain the projectile while the spring expands. When this phase exists, the latch parameters  $R$  and  $v_L$  both reduce the final energy in the projectile as well as increase the latch delay. Once the latch is fully removed, the spring actuation phase begins. At the end of the spring actuation phase, the ballistic phase begins as the projectile is launched.

projection of chameleons [24,25] and cheliceral strikes of trap-jaw spiders [26] are some examples for prey capture. Snapping behaviour observed in snapping shrimp [27,28] and mandible strikes by termite soldiers [29] are used for both predatory evasion and prey capture. Bush crickets [30], locusts, spring-tails and fleas [31] use spring actuation for jumping. Spore ejection/dispersal for species propagation by fern sporangium [32] is yet another example that exemplifies the diverse applications for LaMSA mechanisms in nature.

LaMSA systems are not exclusive to biology. Engineered systems have employed similar mechanisms for over a millennium to achieve high velocities and accelerations, from catapults and Da Vinci's cam-actuated lever [33] to mouse-traps and more modern examples including jumping robots [34–37] and needle-free, spring-powered injectors [38,39].

In all of these systems, a quick transition from potential to kinetic energy enabled by the latch results in power and acceleration outputs greater than what could be achieved by their muscle or actuators alone. Despite the central role that latches play in these systems, there has been a lack of studies regarding the effect of latch parameters on the overall performance of the system [2,5]. As a consequence, latches

have traditionally been viewed as existing in two states: they are either engaged and blocking the release of the spring energy, or released, thereby allowing the spring to freely drive the motion. After all, an instantaneous transition between these two states (latched and unconstrained spring actuated) enables the maximum amount of energy to be released as fast as possible from the spring. As a result, latches in the engineering systems described above [33–36] are designed to transition between the latched and spring actuation phases with no delay, resulting in what we define as an 'instantaneous' latch. In these systems, the effective force on the spring decays to zero before the mass starts to move and is often realized by the use of a contact latch with a sharp edge (zero radius). However, contact-based latches identified in biology do not have sharp edges [40,41]—a difference that is illustrated by figure 2.

While it is challenging for biological systems to achieve sharp edges, this observation raises several questions. Can round latches without sharp edges still behave as an instantaneous latch? What benefits and drawbacks might exist for latches that do not instantaneously transition between the latched and unconstrained spring actuated states? In contrast to instantaneous latches, 'delayed' latches will exhibit an

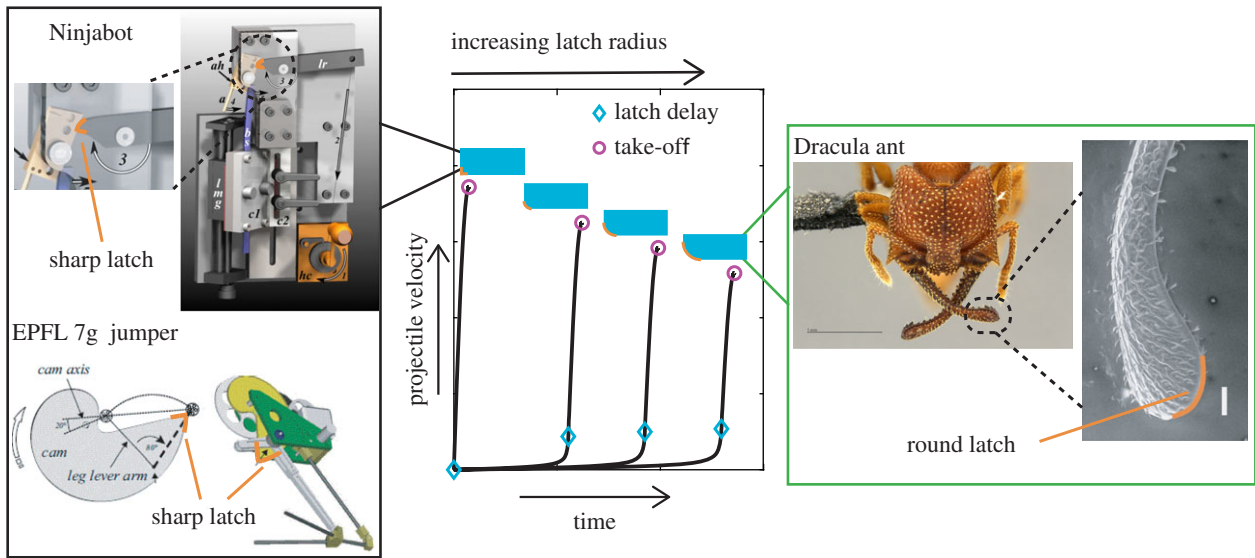


**Figure 2.** The contrast between ‘sharp’ ( $R = 0$ ) engineered latches (images adapted from [15,35]) and an example of a rounded ( $R > 0$ ) contact latch found in biology (Dracula ant head image source: <https://eol.org/pages/489001/media>). The latch radii are highlighted in orange. Engineered LaMSA systems typically use latches with sharp edges and zero radius whereas their biological counterparts have latches with a curvature. Previous work [2] predicts that contact latches with non-zero radius will have output that is both reduced and delayed in comparison to a latch with a sharp edge ( $R = 0$ ).

intermediate state of ‘unlatching’ highlighted in figure 1; in this state, the spring may expand while still constrained by the latch. As shown in figure 2, these delayed latches result in reduced energy output that is also delayed in comparison to an instantaneous latch.

In this work, we use analytical and physical (both engineered and biological) models of the mass–spring–latch system shown in figure 1 to demonstrate that geometrically round latches, such as those found in biology, can behave as both delayed and instantaneous latches. While previous work was grounded on the notion that an instantaneous latch requires the latch to geometrically disappear instantaneously, geometrically round latches without sharp edges can still kinematically disappear instantaneously. In addition, these models indicate that while instantaneous latches release the maximum amount of energy as fast as possible, delayed latches offer more control over the energy output. Controlling the output (e.g. energy release) of these fast systems is extremely challenging [1]; for a fixed spring and spring compression, one would expect a fixed energy output. Using the analytical model developed in [2] and a physical engineering model that resembles the illustration depicted in figure 1, we show the existence of a rich performance space resulting from delayed latches by varying two contact latch parameters: latch radius  $R$  and latch release velocity  $v_L$ . We show that a latch with a large enough radius can attain a range of behaviours, including instantaneous latch behaviour, by simply changing the latch release velocity. A threshold latch velocity is defined as a function of latch radius and other system parameters to delineate instantaneous and delayed latch behaviours.

While the influence of latch parameters is relatively straightforward to study in analytical and engineered systems, the same cannot be said for the wide variety of biological systems. Firstly, latches are internal components in most biological LaMSA systems. This makes it hard to both locate and analyse biological latches. Secondly, it is challenging to systematically change the latch parameters in these systems. Changing geometry would involve small ablations

or additions of material, and varying latch velocity would require muscle stimulation at different rates that correspond to different speeds (a non-trivial task).

The Dracula ant (*Myrmica camillae*) shown in figure 2 poses an interesting biological model given that these organisms use their mandibles as latches, springs, and projectiles [41]. Dracula ants use their mandibles to strike quickly for predation and sometimes for defense. The tips of their mandibles come into contact with each other, and continue to press against one another deforming the mandibles and storing elastic energy. The curved contact area between the two mandibles can be thought of as an approximate latch radius. The rapid energy release occurs when one of the mandibles (the ‘latch’ mandible) slides across the other (the ‘strike’ mandible). We analyse previously published data [42] from Dracula ant (*Myrmica camillae*) strikes to explore variation in output given varying mandible size and latch velocity. The results presented in the analytical, physical, and biological models in this work reinforce the versatility of having a latch with a non-zero radius and support the paradigm of using latches as a control tool in LaMSA systems.

## 2. Material and methods

### 2.1. Mathematical model

A model LaMSA system is illustrated by figure 1. It consists of a projectile mass  $m$  mounted onto a linear spring with stiffness  $k$  compressed by displacement  $\Delta x$ . The natural frequency of the projectile system is defined as  $\omega_n = \sqrt{k/m}$  and will determine the rate at which potential energy is converted to kinetic energy in the unconstrained spring actuation phase of figure 1. The loaded mass–spring pair is held in place by a simplified contact latch defined by two parameters—radius  $R$  and latch release velocity  $v_L$ . Latch radius is defined as the radius of curvature of the edge that is in contact with the mass–spring pair. The potential energy stored in the spring ( $\frac{1}{2}k\Delta x^2$ ) is then released when the latch is removed with a velocity  $v_L$ . The energy conversion from spring potential energy to projectile kinetic energy is mediated by the latch parameters  $R$  and  $v_L$ . This simple model forms the

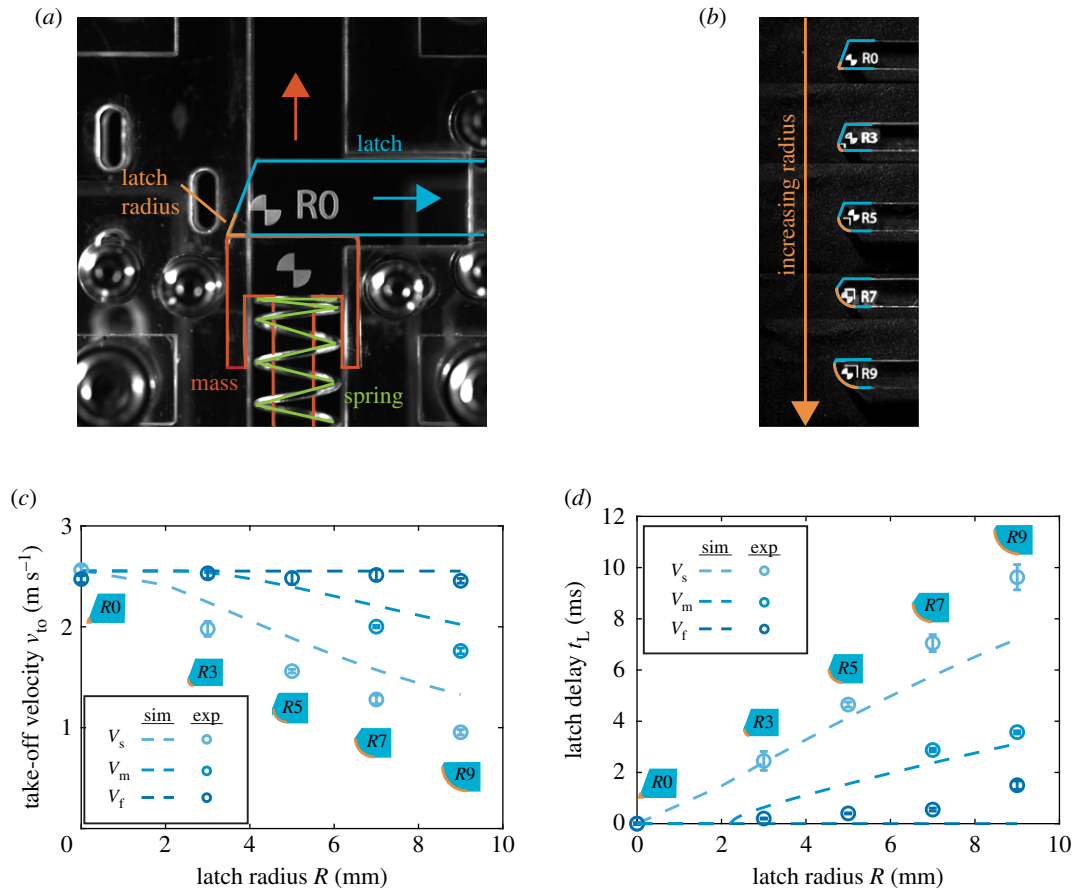


**Figure 3.** The physical model tests the effects of latch velocity and radius on latch delay and take-off velocity. (a) The physical model launches a projectile mass using spring actuation mediated by latches with varying radii and velocities. (b) The latches used in the physical model have latch radii ( $R$ ) ranging from 0 mm (R0) to 9 mm (R9). Latch curvature is highlighted in orange. (c,d) Experimental results (circular markers) and simulation predictions (dashed lines) indicate the take-off velocity  $v_{to}$  of the projectile mass and latch delay  $t_L$  respectively, as  $R$  and  $v_L$  are varied. Each marker and its corresponding error bar represents the mean and standard deviation obtained from a series of four trials. The colour gradient indicates  $v_L$  category: slow ( $v_s$ ), medium ( $v_m$ ) and fast ( $v_f$ ) latch velocity; mean values used for simulations are  $0.96 \text{ m s}^{-1}$ ,  $1.83 \text{ m s}^{-1}$  and  $3.70 \text{ m s}^{-1}$ , respectively. The effect of latch parameters can be observed from the trends seen in both (c) and (d). Higher  $R$  and slower  $v_L$  result in less energy released (i.e. take-off velocity  $v_{to}$ ) and greater latch delay ( $t_L$ ). The influence of  $R$  on  $v_{to}$  and  $t_L$  decreases as  $v_L$  increases demonstrating that rounded latches such as those found in biology can exhibit instantaneous behaviour if pulled away fast enough. Deviations between the experimental and modelling results are most likely due to friction losses at the contact between projectile and latch as well as friction losses at the contact between projectile and bearing surface.

basis of the math model developed and presented in [2], and is further used for simulations presented in this work.

The time at which the latch is no longer constraining the projectile (marked by ‘unlatching-end’ in figure 1) was numerically calculated in MATLAB using the same process as in [2]. This unlatching time was then used to solve for two variables that capture output performance: take-off velocity  $v_{to}$  and latch delay  $t_L$ . Take-off velocity ultimately corresponds to a projectile jump height or kinetic energy recovered from the spring. The time difference between ‘unlatching-start’ and ‘unlatching-end’ in figure 1 is defined as the latch delay,  $t_L$ , as it indicates a delay in unconstrained energy release as compared to an instantaneous latch with  $t_L=0$ . This variable may be of primary importance if the projectile needs to be released quickly, as in an escape jump. Various simulation cases are run by sweeping across the latch design space (varying  $R$  and  $v_L$ ).

## 2.2. Physical model

In order to validate that the mathematical model includes the relevant physics of a real LaMSA system, a physical model that closely resembles the mathematical model was designed and tested. This experimental set-up is shown in figure 3a and consists of a pair of acrylic sheets (McMaster Carr, 1/4" thick) laser cut and assembled to form two perpendicular channels

which accommodate a latch and the projectile. The channels along with three pairs of bearings (McMaster Carr, 60355K501) constrain the motion of the latch and projectile to orthogonal degrees of freedom, illustrated by the turquoise arrow (latch) and the red arrow (projectile). A mass–spring combination is loaded and pre-compressed by a fixed displacement  $\Delta x$  to store the same spring potential energy for each test. A latch holds the projectile in place, and the energy release is triggered by the removal of the latch using a double-acting pneumatic cylinder (FrightProps, HB-2A3M) driven by a solenoid valve (FrightProps, HB-2A0B). Five different latches ( $R=0, 3, 5, 7$  and  $9$  mm) depicted in figure 3b were also laser cut from acrylic (McMaster Carr, 1/4" thick). For a given latch radius, the latch was released at three different speed categories: slow ( $v_s$ ), medium ( $v_m$ ) and fast ( $v_f$ ).

Table 1 lists the parameter values for the mass–spring pair and latches used in the experiments along with the uncertainties measured or calculated. For these parameter values, stored elastic energy is more than 100 times larger than changes in gravitational potential energy, allowing gravity to be safely ignored. Total mass is defined as the mass of the projectile plus the mass of the spring. Table 2 lists the mean values and the corresponding standard deviation of experimental latch velocities measured for each of the latch release categories:  $v_s$ ,  $v_m$  and  $v_f$ .  $v_s$  and  $v_f$  correspond to the slowest and fastest velocities that

**Table 1.** Experimental parameters. Uncertainty for latch release velocities represents the standard deviation of measured velocities during release. Uncertainties for all other parameters are calculated based on the uncertainty of the mass (balance: 100  $\mu\text{g}$ ) and distance (calibrated ruler: 10  $\mu\text{m}$ ). The calculated uncertainties for velocities also use time measurements (10 000 fps imaging: 100  $\mu\text{s}$ ), and are 0.0036  $\text{m s}^{-1}$ , 0.0128  $\text{m s}^{-1}$  and 0.0622  $\text{m s}^{-1}$  for the slow, medium and fast latch velocities, respectively.

parameter	value	uncertainty	units
total mass, $m$	6	0.0001	g
projectile mass	3.75	0.0001	g
spring mass	2.25	0.0001	g
spring stiffness, $k$	2051	55.76	$\text{N m}^{-1}$
natural frequency, $\omega_n$	585	7.95	$\text{rad s}^{-1}$
spring displacement, $\Delta x$	4.37	0.01	mm
latch release velocities, $v_L$	$\bar{v}_s = 0.96$	0.056	$\text{m s}^{-1}$
	$\bar{v}_m = 1.83$	0.027	$\text{m s}^{-1}$
	$\bar{v}_f = 3.70$	0.098	$\text{m s}^{-1}$
latch radius, $R$	0, 3, 5, 7, 9	0.01	mm

can reliably be achieved using the pneumatic actuation set-up controlled by the solenoid valve.  $v_m$  corresponds to a velocity lying in between  $v_s$  and  $v_f$ . More information on latch speed and measurement is provided in the electronic supplementary material. For  $v_s$  and  $v_f$ , experiments were performed with all of the latches. For  $v_m$ , experiments were recorded only for 7 and 9 mm radius latches to provide some additional points at these larger radii. Each experiment using a given combination of  $R$  and  $v_L$  consists of four trials.

The experiments were recorded with a Photron AX-200 high-speed camera (pixel resolution:  $896 \times 768$ , calibrated ruler described in table 1) at 10 000 fps (shutter duration: 1/60 000 s) and both latch motion and projectile motion were analysed using tracking software (Image Systems, TEMA). Take-off velocity was calculated from these images at the point when the spring and mass separated from the substrate. Example videos of releases with varying latch speed and radii are provided in the electronic supplementary material.

Measuring latch delay was more challenging. In theory, the point of maximum projectile acceleration should equate to the instant at which latch force goes to zero, but this was not the case in the physical system (electronic supplementary material, figures S1 and S2). Instead, latch delay was measured when physical separation was visually observed between the projectile and the latch. While this method is expected to slightly overpredict delay, it provided consistent results.

### 2.3. Dracula ant data

Mandible tip position data captured on high-speed video from two types of Dracula ants (larger major and smaller minor workers) was made available in [42]. This dataset provides  $x$ - $y$  coordinates of the mandible tips for each frame along with the camera frame rate. Four ants of each type were analysed over 4–5 strikes per ant as available in the dataset. The first mandible to move during each strike was designated as the latch mandible, and unlatching time was defined as the time difference between the start of latch mandible and strike mandible motion. Average latch mandible velocity was calculated as the angle over which the latch mandible displaced before the strike mandible began to move, divided by the unlatching time. The maximum strike

velocity was calculated using the maximum angular motion of the strike mandible between two frames and dividing by the time interval between frames. An example of this  $x$ - $y$  data for five strikes from one of the major worker ants along with the mandible angular position versus time is provided in electronic supplementary material, figure S4.

Even though this biological model is not perfectly analogous to the mathematical model and physical model, it is a first and foundational analysis of contact latch release in biology. This study builds on recent work in the Dracula ant [41] and click beetle [43] that has focused on understanding latch morphology and mechanical properties. By examining the association between latch and strike velocity, we assessed whether changes in latch velocity correlate with changes in strike velocity to indicate changes between instantaneous and delayed latch behaviour.

## 3. Results and discussion

Previous work on LaMSA systems realized instantaneous latch behaviour with a latch that geometrically disappeared instantaneously when pulled away [2]. In the physical model experiments and simulation results (figure 3*c,d*), this geometrically instantaneous latch is represented by  $R=0$ . As can be seen, take-off velocity and delay do not change with latch removal speed due to the instantaneous transition between the latched and spring actuation phases enabled by geometry (figure 1). As expected, this instantaneous latch behaviour provides the maximum energy return with zero delay.

Conventional wisdom also dictates that a larger radius latch reduces take-off velocity and increases delay [2]. However, these results make it clear that even large radius latches exhibit instantaneous behaviour when they are pulled at the fastest velocity ( $v_f$ ). Take-off velocity remains the same as seen in the  $R=0$  case despite increasing radius, and latch delay stays close to zero. This result makes it clear that instantaneous latch behaviour is a result of kinematic constraints, and not limited to a subset of geometries with sharp edges.

In addition, these results demonstrate that latch parameters (latch radius and release velocity) can be used to control the projectile take-off velocity. For a non-zero radius latch, the projectile take-off velocity can be controlled through latch release velocity. Similarly, for a given latch release velocity, the projectile take-off velocity can be controlled through latch radius. Given that it is relatively simple to vary the latch velocity with an actuator, especially in engineering systems, the remaining discussion will focus on using latch release velocity as the control input. Controlling energy output of LaMSA systems is extremely challenging once energy is stored. However, these results indicate that even if energy is already stored in a system, output performance can still be controlled by the latch, albeit using a feedforward approach. If a large jump or fast strike is required, a system can use an instantaneous latch by pulling its latch away fast enough. If the output needs to be arrested or reduced after energy has been stored, a low latch release velocity will accomplish this in latches with non-zero radius. In addition, a larger latch radius affords a larger range of performance output pointing to a significant benefit to having non-zero radii latches in both biological and engineering systems.

The output control afforded by delayed latch behaviour does have trade-offs. As indicated by the name ‘delayed latch’, latch delay  $t_L$  increases due to the addition of the unlatching phase seen in figure 1 resulting in a slower projectile take-off. If a fast response to a trigger is required (e.g. an escape response), it will be important to provide

**Table 2.** Latch velocities  $v_L$  measured during the experiments.  $v_s$ ,  $v_m$  and  $v_f$  denote the mean latch release velocities attained during the unlatching event for a given latch radius.  $\sigma_s$ ,  $\sigma_m$  and  $\sigma_f$  denote the corresponding standard deviation over the course of unlatching. The subscripts  $s$ ,  $m$  and  $f$  represent the latch release categories: slow, medium and fast, respectively.

$R$ (mm)	$v_L$ (m s <sup>-1</sup> )						
	$v_L^{\text{thresh}}$	$v_s$	$\sigma_s$	$v_m$	$\sigma_m$	$v_f$	$\sigma_f$
0	0	0.97	0.072	—	—	3.72	0.036
3	2.12	1.07	0.091	—	—	3.7	0.097
5	2.73	0.93	0.021	—	—	3.61	0.092
7	3.24	0.93	0.031	1.84	0.031	4.08	0.165
9	3.67	0.90	0.024	1.81	0.022	3.40	0.059
mean value used for simulations		0.96		1.83		3.70	

instantaneous latch behaviour to minimize delay. Delayed latches also result in efficiency losses. Only a fraction of the spring energy is used to generate unconstrained motion in the projectile due to the fact that some energy is released from the spring while still geometrically constrained by the latch in the unlatching phase. The deviation between modelled and experimental results also increases for delayed latches, likely due to increased frictional losses between the latch and the projectile from longer periods of contact.

### 3.1. Threshold latch velocity

The results in figure 3*c,d* also make it clear that at each radius, there must be a threshold latch velocity above which the latch exhibits instantaneous behaviour, and below which the latch acts as a delayed latch. As seen from both experiments and simulations for a given  $R > 0$ ,  $v_{to}$  increases as  $v_L$  is increased and eventually exhibits instantaneous behaviour when the latch is released quickly enough. Similarly, for a given latch velocity there is a threshold radius below which instantaneous latch behaviour is observed, and above which delayed latch behaviour is observed. This result is most clearly seen by the ‘kink’ in the lines representing simulation data in figure 3*c,d* where take-off velocity and latch delay start to deviate from the instantaneous results. Because it is generally simpler to vary velocity than radius in a physical system, we will examine the threshold velocity, henceforth defined as the threshold latch velocity  $v_L^{\text{thresh}}$ , as a boundary between instantaneous and delayed latch behaviours.

Threshold latch velocity defines the velocity at which the kinematic constraint of the latch on the projectile disappears instantaneously. This kinematic disappearance will depend on latch radius, but also on the projectile and spring parameters. A mass–spring system with a high natural frequency requires a faster latch so that the latch constraint decays to zero before the spring starts to expand. Equation (3.1) defines  $v_L^{\text{thresh}}$  mathematically and is derived from the mathematical model described in [2] (more detail on the derivation is provided in the electronic supplementary material). If  $v_L \geq v_L^{\text{thresh}}$ , the latch is instantaneous irrespective of its radius. For latch release velocities slower than this threshold velocity ( $v_L < v_L^{\text{thresh}}$ ), the delayed latch behaviour results in a rich performance space where the latch parameters, radius  $R$

and the latch release velocity  $v_L$ , control the output performance  $v_{to}$  and  $t_L$ .

$$v_L^{\text{thresh}} = \sqrt{\Delta x R \frac{k}{m}}. \quad (3.1)$$

In the physical model experiments,  $v_f > v_L^{\text{thresh}}$  for all latches other than the 9 mm latch as can be seen from table 2. In figure 3*c,d*, the performance begins to deviate from ideal for the 9 mm latch and this deviation can be seen most clearly in figure 3*d*. All of the other latch radii exhibit instantaneous behaviour for the  $v_f$  case. As latch velocity slows, take-off velocity also slows for the 5 and 7 mm latches due to the fact that these latch velocities result in delayed latch behaviour.

### 3.2. Effect of different system parameters on threshold velocity

As described by equation (3.1),  $v_L^{\text{thresh}}$  is directly proportional to the square root of the latch radius and spring compression. Therefore, for a fixed  $k$  and  $m$ ,  $v_L^{\text{thresh}}$  is higher for a latch with larger  $R$  or more stored energy.  $v_L^{\text{thresh}}$  is also directly proportional to the natural frequency of the system ( $\omega_n = \sqrt{k/m}$ ). For a given spring stiffness,  $v_L^{\text{thresh}}$  increases as the system mass decreases and vice versa. Thus, for heavier systems, this threshold velocity is lower and latch parameters have less influence on the output. In part, this is because the entire projectile system is slower. These relationships are further illustrated by figure 4*a*, which shows a colour map depicting how  $v_L^{\text{thresh}}$  varies for different latch radii and system natural frequencies given a fixed  $\Delta x$ .

Two natural frequencies were chosen to represent a hypothetical fast (high frequency) and a slow (low frequency) system, marked by orange triangles and blue circles respectively. Assuming a similar spring stiffness, fast systems are equivalent to low-mass projectiles like insects. Notably in figure 4*a*,  $v_L^{\text{thresh}}$  is higher for fast versus slow systems. Because the unconstrained spring expansion is fast, the latch needs to move out of the way faster to kinematically disappear instantaneously. As a consequence, there is also a much larger latch velocity range defining the delayed latch behaviour, and hence, a rich performance space exists to influence the system’s output performance. In slower systems, this performance space shrinks due to the decrease in  $v_L^{\text{thresh}}$ .

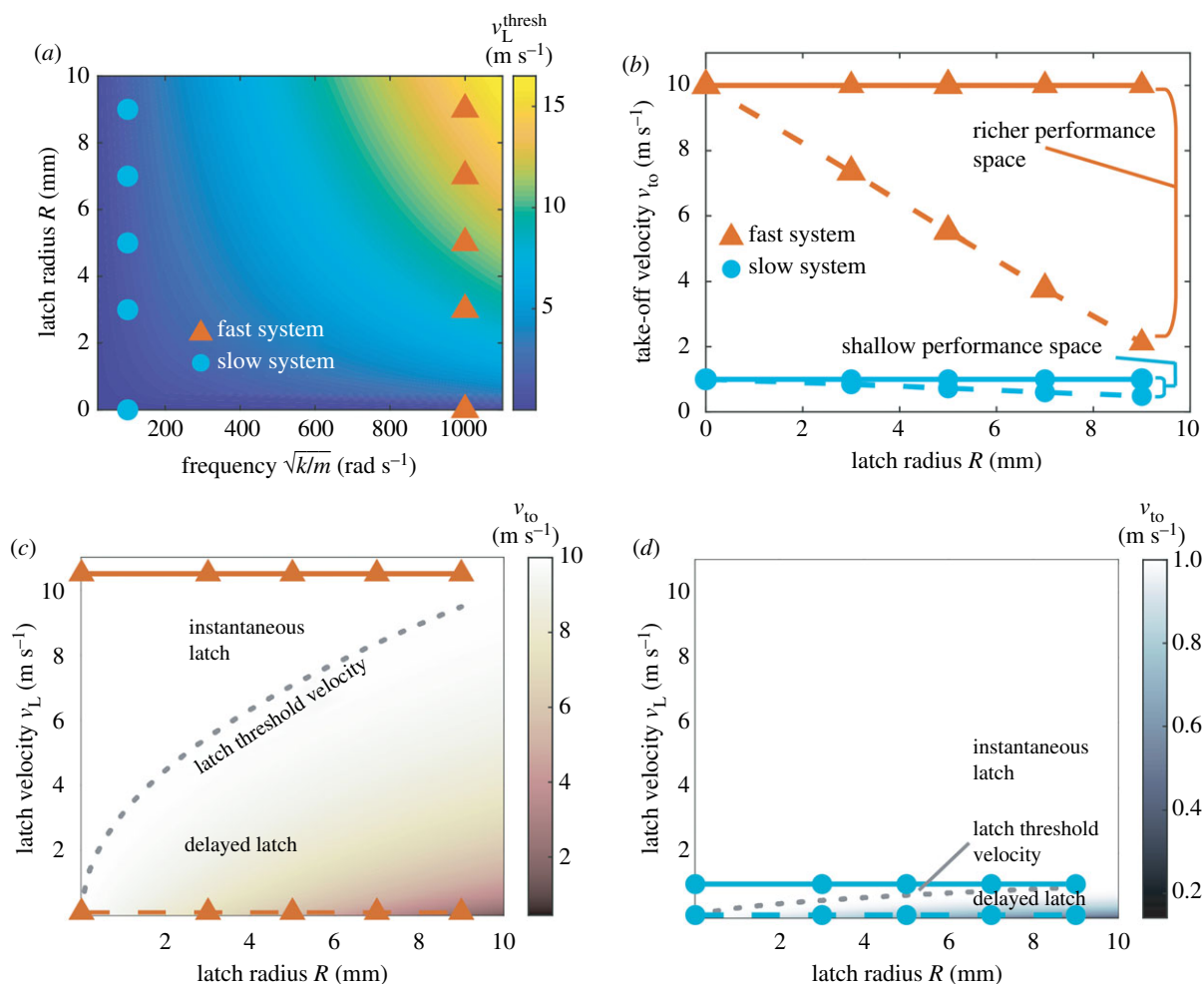


**Figure 4.** If the latch is moved away faster than the threshold latch velocity ( $v_L^{\text{thresh}}$ ), then the latch behaves as an instantaneous latch. If the latch moves more slowly, the unlatching phase exists and the latch is delayed.  $v_L^{\text{thresh}}$  is a function of the system's natural frequency, latch radius, and spring displacement. (a) Fast projectile systems (orange triangles,  $\omega_n = 1000$  m s<sup>-1</sup>) have higher latch threshold velocities  $v_L^{\text{thresh}}$  than slower projectile systems (blue circles,  $\omega_n = 100$  m s<sup>-1</sup>) across varying radii. (b) As a result of the higher  $v_L^{\text{thresh}}$ , fast systems also exhibit a larger performance space for latch-based tuning of take-off velocity ( $v_{\text{to}}$ ) than slower systems when operating below  $v_L^{\text{thresh}}$  (dashed line). The solid lines indicate simulations run above  $v_L^{\text{thresh}}$  showing maximum take-off velocity due to instantaneous latch behaviour. Latch parameters ( $R$  and  $v_L$ ) can have a greater influence on the output ( $v_{\text{to}}$ ) for faster systems than slower ones. (c) and (d) depict the performance ( $v_{\text{to}}$ ) heat-map for the fast and slow systems respectively. The solid and dashed lines reflect the same latch velocities chosen for (b):  $v_L > v_L^{\text{thresh}}$  and  $v_L < v_L^{\text{thresh}}$ , respectively. The dotted line illustrates the relationship between threshold latch velocity and latch radius. The performance space ( $v_{\text{to}}$ ) is richer for faster systems because a higher  $v_L^{\text{thresh}}$  means that a larger range of latch velocity can be used before instantaneous behaviour is observed.

Figure 4c,d illustrates a heat map of the take-off velocity for the same fast ( $\omega_n = 1000$  rad s<sup>-1</sup>) and slow ( $\omega_n = 100$  rad s<sup>-1</sup>) systems from figure 4a,b. They show the range of performance space attainable for delayed latch behaviour as well as the latch velocity required to achieve instantaneous behaviour. This reinforces the earlier results that latches with non-zero radius can attain a range of behaviours, both instantaneous and delayed, by simply controlling the rate at which the latch is released. Furthermore, latches play a more prominent role in fast, often lightweight, systems than slow systems.

### 3.3. Dracula ant

Both instantaneous and delayed latch behaviours are also seen in biological systems. The influence of latch velocity on the performance of a biological system is illustrated in figure 5, which depicts maximum strike velocities plotted against the corresponding average latch velocities for two subcategories of Dracula ants: major (larger ants, teal stars) and minor (smaller ants, navy blue squares) workers. For major workers, slower latch velocities result in slower strikes. In other words, these ants exhibit a

delayed latch behaviour in which latch velocity affects the performance. On the other hand, the strikes of minor workers are agnostic to latch velocity; output is stereotyped as expected from an instantaneous latch. This implies that the latch release velocities used by minor workers are above  $v_L^{\text{thresh}}$ .

While major worker ants exhibit a delayed latch behaviour and minor worker ants exhibit instantaneous latch behaviour, it is unclear if the threshold latch velocity can be directly compared between the two types of ants. Some simplifications can be made to draw conclusions about threshold latch velocity for the ant mandibles. We start by assuming that the spring displacement is linear due to the small angle deflection of the mandibles during bending, and the mandibles are treated as cantilever beams with spring stiffness ( $k = 3EI/l_m^3$ , where  $E$  is Young's modulus,  $I$  is the second moment of area, and  $l_m$  is the mandible length). Scaling all lengths by  $\lambda$  results in  $R \propto \lambda^1$ ,  $k \propto (\lambda^0 \lambda^4 / \lambda^3) = \lambda^1$ ,  $\Delta x \propto \lambda^1$  and  $m \propto \lambda^3$ .

$$v_L^{\text{thresh}} \propto \sqrt{\lambda^1 \lambda^1 \frac{\lambda^1}{\lambda^3}} \propto \lambda^0. \quad (3.2)$$

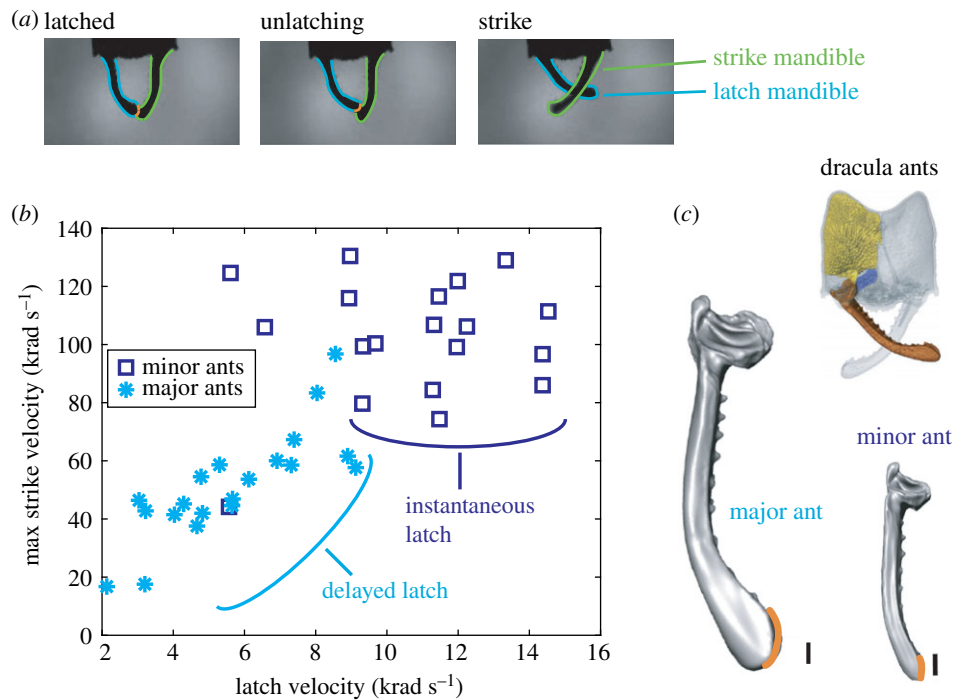


**Figure 5.** Dracula ants (*Myrmica camillae*) use a LaMSA mechanism with a contact latch to load and release their mandibles. (a) Elastic energy is loaded into their mandibles by pressing their tips together and released when one of the mandibles (latch mandible) slides off of the surface of the other (strike mandible). The curved contact area (highlighted in orange) between the mandible tips serves as the contact latch. (b) The velocity of the latch mandible and strike mandible were analysed using previously published data [42] from major (stars) and minor (squares) worker ants. These results indicate that minor workers may be using latch velocities above a threshold latch velocity since strike velocity is agnostic to latch velocity, which is the definition of instantaneous latch behaviour. Conversely, latch velocity correlates to strike velocity for major workers indicating delayed latch behaviour. (c) Scale bars next to the major and minor ant mandibles represent 0.1 mm, and mandible images were adapted from [41].

In this case, the threshold latch velocity is scale independent and should be approximately the same regardless of ant type. While the mandible models from [41] in figure 5 are not geometrically similar as assumed, this analysis does support the idea that  $v_L^{\text{thresh}} \approx 8 \text{krad s}^{-1}$ , and major workers move their latch mandibles at velocities below the threshold while minor workers use latch velocities above  $v_L^{\text{thresh}}$ . Ultimately, the current mathematical model could be modified to better capture the dynamics of this specific ant species to further explore unlatching in the Dracula ant.

### 3.4. Implications for control of latch-mediated spring actuation systems

One of the striking conclusions of this work is that latches with non-zero radius, as found in biology, can exhibit both instantaneous latch behaviours (in which a maximum amount of energy is released as fast as possible) as well as delayed latch behaviours (in which latch velocity controls the system performance). Previous engineering efforts to design geometrically instantaneous latches with  $R=0$  provide no pathway to control energy output once the spring has been loaded. Instead, a non-zero latch radius combined with variable release velocity provides a feedforward means to control energy output in both biological and engineered systems. Many systems, especially engineered systems like jumping robots (e.g. [35,36]), have a fixed spring compression built into the design. These robots jump with the same take-off velocity every time because they use a geometrically instantaneous latch to release the maximum amount of energy. Using a latch with  $R>0$  and controlling the latch speed in these robots could provide a means for these

robots to jump varying distances. If the latch motor is fast enough and strong enough, the robot can cover a full range of jump distances from zero to its maximum jump height/distance defined by energy stored in its spring.

In biology, latches have typically received scattered attention in the literature and the results of this study suggest that the role of latches in behaviour and control warrants new attention. Biological diversity of latches includes variation in latch morphology, control, and mechanics. Multiple studies have previously suggested, but not tested, how different biological latch mechanisms may enable variable or controlled outputs in various organisms [3,7,21,27,28,31,44–50]. For example, mantis shrimp and locusts have contact latches that are integrated into the structure of the flexor muscle apodemes and are released by relaxing the flexor muscles [18,40,51–53]. While the morphology of these latches has been imaged, the connection between surface mechanics, morphology, and release velocity has not yet been analysed. This is because, as mentioned previously, a major challenge in analysing these contact latch systems in biology are that they are internal, and thus difficult to visualize while releasing. However, in addition to the Dracula ants in this study [42], there are animals that use external latches, such as the adhesive latches of jumping gall midge larvae [21], other species of trap-jaw ants [9,54], click beetles [43,55–57], and possibly froghopper insects [46]. These external latch systems will enable future analysis of the biological latch dynamics, latch release velocity, and their association with uses across different environments and behaviours.

In addition, the results of this study point to a possible trade-off that could be exploited in both natural and engineered systems. By definition, systems with delayed latch behaviour

spend more time in the unlatching phase of figure 1. This increased time before unconstrained spring actuation could give systems more time to abort their energy release through a rapid change in latch velocity. As mentioned previously, it is especially challenging to control the release of energy if needed after this process has begun, but biological systems can do this when needed [48]. While these systems would trade off take-off velocity for this additional delay, this added control benefit may be worth it. Control through latch design and release offers an interesting new control technique for LaMSA systems.

**Data accessibility.** The data and code supporting the findings of this study are available from the Dryad Digital Repository: <https://doi.org/10.5061/dryad.fttdz08pb> [58].

## References

- Longo SJ, Cox SM, Azizi E, Ilton M, Olberding JP, St Pierre R, Patek SN. 2019 Beyond power amplification: latch-mediated spring actuation is an emerging framework for the study of diverse elastic systems. *J. Exp. Biol.* **222**, jeb197889. <https://doi.org/10.1242/jeb.197889>.
- Ilton M *et al.* 2018 The principles of cascading power limits in small, fast biological and engineered systems. *Science* **360**, eaao1082. (doi:10.1126/science.aao1082)
- Liu F, Chavez RL, Patek SN, Pringle A, Feng JJ, Chen C-H. 2017 Asymmetric drop coalescence launches fungal ballistospores with directionality. *J. R. Soc. Interface* **14**, 20170083. (doi:10.1098/rsif.2017.0083)
- Koh J, Jung S, Wood RJ, Cho K. 2013 A jumping robotic insect based on a torque reversal catapult mechanism. In *2013 IEEE/RSJ Int. Conf. on Intelligent Robots and Systems*, pp. 3796–3801.
- Abbott EM, Nezwek T, Schmitt D, Sawicki GS. 2019 Hurry up and get out of the way! Exploring the limits of muscle-based latch systems for power amplification. *Integr. Comp. Biol.* **59**, 1546–1558. (doi:10.1093/icb/icz141)
- Olberding JP, Deban SM, Rosario MV, Azizi E. 2019 Modeling the determinants of mechanical advantage during jumping: consequences for spring- and muscle-driven movement. *Integr. Comp. Biol.* **59**, 1515–1524. (doi:10.1093/icb/icz139)
- Gronenberg W, Ehmer B. 1996 The mandible mechanism of the ant genus *Anochetus* (Hymenoptera, Formicidae) and the possible evolution of trap-jaws. *Zoology* **99**, 153–162.
- Patek SN, Baio JE, Fisher BL, Suarez AV. 2006 Multifunctionality and mechanical origins: ballistic jaw propulsion in trap-jaw ants. *Proc. Natl Acad. Sci. USA* **103**, 12787–12792. (doi:10.1073/pnas.0604290103)
- Larabee F, Suarez A. 2014 The evolution and functional morphology of trap-jaw ants (Hymenoptera: Formicidae). *Myrmecological News* **20**, 25–36.
- Larabee FJ, Gronenberg W, Suarez AV. 2017 Performance, morphology and control of power-amplified mandibles in the trap-jaw ant *Myrmoteras* (Hymenoptera: Formicidae). *J. Exp. Biol.* **220**, 3062–3071. (doi:10.1242/jeb.156513)
- Spagna JC, Schelkopf A, Carrillo T, Suarez AV. 2009 Evidence of behavioral co-option from context-dependent variation in mandible use in trap-jaw ants (*Odontomachus* spp.). *Naturwissenschaften* **96**, 243–250. (doi:10.1007/s00114-008-0473-x)
- Zhakypov Z, Mori K, Hosoda K, Paik J. 2019 Designing minimal and scalable insect-inspired multi-locomotion millirobots. *Nature* **571**, 381–386. (doi:10.1038/s41586-019-1388-8)
- Gibson JC, Larabee FJ, Touchard A, Orivel J, Suarez AV. 2018 Mandible strike kinematics of the trap-jaw ant genus *Anochetus* Mayr (Hymenoptera: Formicidae). *J. Zool.* **306**, 119–128. (doi:10.1111/jzo.12580)
- McHenry MJ, Anderson PSL, Van Wassenbergh S, Matthews DG, Summers AP, Patek SN. 2016 The comparative hydrodynamics of rapid rotation by predatory appendages. *J. Exp. Biol.* **219**, 3399–3411. (doi:10.1242/jeb.140590)
- Cox SM, Schmidt D, Modarres-Sadeghi Y, Patek SN. 2014 A physical model of the extreme mantis shrimp strike: kinematics and cavitation of ninjabot. *Bioinspir. Biomim.* **9**, 016014. (doi:10.1088/1748-3182/9/1/016014)
- Patek SN. 2019 The power of mantis shrimp strikes: interdisciplinary impacts of an extreme cascade of energy release. *Integr. Comp. Biol.* **59**, 1573–1585. (doi:10.1093/icb/icz127)
- Patek SN, Korff WL, Caldwell RL. 2004 Deadly strike mechanism of a mantis shrimp. *Nature* **428**, 819–820. (doi:10.1038/428819a)
- Burrows M. 1969 The mechanics and neural control of the prey capture strike in the mantid shrimps *Squilla* and *Hemisquilla*. *Zeitschrift für Vergleichende Physiologie* **62**, 361–381. (doi:10.1007/BF00299261)
- Burrows M. 2006 Jumping performance of frog hopper insects. *J. Exp. Biol.* **209**, 4607–4621. (doi:10.1242/jeb.02539)
- Goetzke HH, Patrick JG, Federle W. 2019 Frog hoppers jump from smooth plant surfaces by piercing them with sharp spines. *Proc. Natl Acad. Sci. USA* **116**, 3012–3017. (doi:10.1073/pnas.1814183116)
- Farley GM, Wise MJ, Harrison JS, Sutton GP, Kuo C, Patek SN. 2019 Adhesive latching and legless leaping in small, worm-like insect larvae. *J. Exp. Biol.* **222**, jeb201129. (doi:10.1242/jeb.201129)
- Forterre Y, Skotheim JM, Dumais J, Mahadevan L. 2005 How the Venus flytrap snaps. *Nature* **433**, 421–425. (doi:10.1038/nature03185)
- Nüchter T, Benoit M, Engel U, Özbek S, Holstein TW. 2006 Nanosecond-scale kinetics of nematocyst discharge. *Curr. Biol.* **16**, R316–R318. (doi:10.1016/j.cub.2006.03.089)
- de Groot JH, van Leeuwen JL. 2004 Evidence for an elastic projection mechanism in the chameleon tongue. *Proc. R. Soc. B* **271**, 761–770. (doi:10.1098/rspb.2003.2637)
- Müller UK, Kranenbarg S. 2004 Power at the tip of the tongue. *Science (New York, N.Y.)* **304**, 217–9. (doi:10.1126/science.1097894)
- Wood H, Parkinson D, Griswold C, Gillespie R, Elias D. 2016 Repeated evolution of power-amplified predatory strikes in trap-jaw spiders. *Curr. Biol.* **26**, 1057–1061. (doi:10.1016/j.cub.2016.02.029)
- Ritzmann R. 1973 Snapping behavior of the shrimp *Alpheus californiensis*. *Science* **181**, 459–460. (doi:10.1126/science.181.4098.459)
- Ritzmann RE. 1974 Mechanisms for the snapping behavior of two alpheid shrimp, *Alpheus californiensis* and *Alpheus heterochelis*. *J. Comp. Physiol.* **95**, 217–236. (doi:10.1007/BF00625445)
- Seid MA, Scheffrahn RH, Niven JE. 2008 The rapid mandible strike of a termite soldier. *Curr. Biol.* **18**, R1049–R1050. (doi:10.1016/j.cub.2008.09.033)
- Burrows M, Morris O. 2003 Jumping and kicking in bush crickets. *J. Exp. Biol.* **206**, 1035–1049. (doi:10.1242/jeb.00214)
- Gronenberg W. 1996 Fast actions in small animals: springs and click mechanisms. *J. Comp. Physiol. A* **178**, 727–734. (doi:10.1007/BF00225821)
- Noblin X, Rojas NO, Westbrook J, Llorens C, Argentina M, Dumais J. 2012 The fern sporangium: a unique catapult. *Science (New York, N.Y.)* **335**, 1322. (doi:10.1126/science.1215985)
- Moon FC. 2007 The machines of Leonardo da Vinci and Franz Reuleaux. In *History of mechanism and machine science*. Dordrecht, The Netherlands: Springer. (doi:10.1007/978-1-4020-5599-7)

34. Zaitsev V, Gvirzman O, Ben Hanan U, Weiss A, Ayali A, Kosa G. 2015 A locust-inspired miniature jumping robot. *Bioinspir. Biomim.* **10**, 066012. (doi:10.1088/1748-3190/10/6/066012)
35. Kovač M, Fuchs M, Guignard A, Zufferey J-C, Floreano D. 2008 A miniature 7g jumping robot. In *IEEE Int. Conf. on Robotics and Automation*, pp. 373–378.
36. Burdick J, Fiorini P. 2003 Minimalist jumping robots for celestial exploration. *Int. J. Rob. Res.* **22**, 653–674. (doi:10.1177/02783649030227013)
37. Noh M, Kim S, An S, Koh J, Cho K. 2012 Flea-inspired catapult mechanism for miniature jumping robots. *IEEE Trans. Rob.* **28**, 1007–1018. (doi:10.1109/TR0.2012.2198510)
38. Pharmajet. Needle-free injection technology. <https://pharmajet.com/> (accessed 02 August 2019).
39. Schoubben A, Cavicchi A, Barberini L, Faraon A, Berti M, Ricci M, Blasi P, Postriotti L. 2015 Dynamic behavior of a spring-powered micronozzle needle-free injector. *Int. J. Pharm.* **491**, 91–98. (doi:10.1016/j.ijpharm.2015.05.067)
40. Patek SN, Nowroozi BN, Baio JE, Caldwell RL, Summers AP. 2007 Linkage mechanics and power amplification of the mantis shrimp's strike. *J. Exp. Biol.* **210**, 3677–88. (doi:10.1242/jeb.006486)
41. Larabee FJ, Smith AA, Suarez AV. 2018 Snap-jaw morphology is specialized for high-speed power amplification in the dracula ant, *Mystrium camillae*. *R. Soc. Open Sci.* **5**, 181447. (doi:10.1098/rsos.181447)
42. Larabee FJ, Smith AA, Suarez AV. 2018 Data from: Snap-jaw morphology is specialized for high-speed power amplification in the Dracula ant, *Mystrium camillae*. Dryad Digital Repository. (doi:10.5061/dryad.4863215)
43. Bolmin O, Wei L, Hazel AM, Dunn AC, Wissa A, Alleyne M. 2019 Latching of the click beetle (Coleoptera: Elateridae) thoracic hinge enabled by the morphology and mechanics of conformal structures. *J. Exp. Biol.* **222**, jeb196683. (doi:10.1242/jeb.196683)
44. Gronenberg W. 1996 The trap-jaw mechanism in the dacetine ants *Daceton armigerum* and *Strumigenys* sp. *J. Exp. Biol.* **199**, 2021–2033.
45. Anker A, Ah Yong ST, Noel PY, Palmer AR. 2006 Morphological phylogeny of alpheid shrimps: parallel preadaptation and the origin of a key morphological innovation, the snapping claw. *Evolution* **60**, 2507–2528. (doi:10.1111/j.0014-3820.2006.tb01886.x)
46. Burrows M. 2006 Morphology and action of the hind leg joints controlling jumping in froghopper insects. *J. Exp. Biol.* **209**, 4622–4637. (doi:10.1242/jeb.02554)
47. Cofer D, Cymbalyuk G, Heitler WJ, Edwards DH. 2010 Neuromechanical simulation of the locust jump. *J. Exp. Biol.* **213**, 1060–1068. (doi:10.1242/jeb.034678)
48. Kagaya K, Patek S. 2016 Feed-forward motor control of ultrafast, ballistic movements. *J. Exp. Biol.* **219**, 319–333. (doi:10.1242/jeb.130518)
49. Kaji T, Anker A, Wirkner CS, Palmer AR. 2018 Parallel saltational evolution of ultrafast movements in snapping shrimp claws. *Curr. Biol.* **28**, 106–113.e4. (doi:10.1016/j.cub.2017.11.044)
50. Patek S, Longo SJ. 2018 Evolutionary biomechanics: the pathway to power in snapping shrimp. *Curr. Biol.* **28**, R115–R117. (doi:10.1016/j.cub.2017.12.033)
51. Burrows M, Hoyle G. 1972 Neuromuscular physiology of the strike mechanism of the mantis shrimp, *Hemisquilla*. *J. Exp. Zool.* **179**, 379–393. (doi:10.1002/jez.1401790309)
52. McNeill P, Burrows M, Hoyle G. 1972 Fine structure of muscles controlling the strike of the mantis shrimp, *Hemisquilla*. *J. Exp. Zool.* **179**, 395–415. (doi:10.1002/jez.1401790310)
53. Bennet-Clark H. 1975 The energetics of the jump of the locust *Schistocerca gregaria*. *J. Exp. Biol.* **63**, 53–83.
54. Gronenberg W, Brandão CRF, Dietz BH, Just S. 1998 Trap-jaws revisited: the mandible mechanism of the ant *Acanthognathus*. *Physiol. Entomol.* **23**, 227–240. (doi:10.1046/j.1365-3032.1998.233081.x)
55. Evans MEG. 1973 The jump of the click beetle (Coleoptera: Elateridae)—energetics and mechanics. *J. Zool.* **169**, 181–194. (doi:10.1111/j.1469-7998.1973.tb04553.x)
56. Ribak G, Weihs D. 2011 Jumping without using legs: the jump of the click-beetles (Elateridae) is morphologically constrained. *PLoS ONE* **6**, 1–7. (doi:10.1371/journal.pone.0020871)
57. Ribak G, Reingold S, Weihs D. 2012 The effect of natural substrates on jump height in click-beetles. *Funct. Ecol.* **26**, 493–499. (doi:10.1111/j.1365-2435.2011.01943.x)
58. Divi S, Ma X, Ilton M, St. Pierre R, Eslami B, Patek SN, Bergbreiter S. 2020 Data from: Latch-based control of energy output in spring actuated systems. Dryad Digital Repository. (<https://doi.org/10.5061/dryad.fttdz08pb>)